

## **Time-dependent quantum dynamics of reactive scattering and the calculation of product quantum state distributions – A study of the collinear $F + H_2(v = 0) \rightarrow HF(v') + H$ reaction**

**C. Clay Marston\*, Gabriel G. Balint-Kurti, and Richard N. Dixon**

School of Chemistry, University of Bristol, Bristol, BS8 1TS, UK

Received October 17, 1990/Accepted November 13, 1990

**Summary.** A new method for the calculation of partial cross sections in the time-dependent quantum theory of molecular reactive scattering processes is discussed. Preliminary calculations are presented which clearly illustrate the power of the method. They show how all the partial cross sections associated with a single initial quantum state may be computed over a very wide energy range from a single propagation of a prepared wavepacket. The resonance behaviour is obtained without difficulty and the energies of the reactive scattering resonances are exactly reproduced.

**Key words:** Partial cross sections – Time-dependent quantum theory – Resonance behaviour – Reactive scattering resonances

### **1. Introduction**

Time-dependent quantum dynamics has now been used for a number of years to calculate photodissociation cross sections [1–9] and the other observable attributes of molecular photodissociation processes. These observables include in particular the final quantum state distributions of the molecular photofragments of the breakup process and the emission spectrum of the molecule during dissociation (the resonance Raman spectrum) [10]. A break-through in the application of time-dependent quantum dynamical techniques to molecular dynamics and collision processes was made in the work of Kosloff [11–14]. He showed how the fast Fourier transform technique could be used to efficiently compute the derivatives of the wavefunction needed in the application of the kinetic energy operator. He, and others before him, have also discussed [7, 14, 15] how the essential step in performing time-dependent quantum dynamical calculations is the action of the hamiltonian operator on a well-specified wavefunction. If this elementary step can be achieved, then the time-dependent Schrödinger equation can be successfully solved.

The difficult part of acting with the hamiltonian operator on a wavefunction is associated with the derivative operators in the kinetic energy part of the

\* *Present address:* Department of Chemistry, Kansas State University, Manhattan, Kansas 66506, USA

hamiltonian operator. The kinetic energy operator is nonlocal in the coordinate representation or Schrödinger picture, but is local in the momentum representation [16]. Kosloff's methods utilise the convenience of the momentum representation for the evaluation of the kinetic energy operator. The Fourier transforms which are performed are in effect transforming the wavefunction to the momentum representation and back again. In previous work [9, 10] the authors have applied time-dependent quantum dynamical techniques to molecular photodissociation processes. As part of this research they have developed a new method for analysing the time-dependent wavepacket [9] and for extracting from it the probabilities for the formation of specific quantum states of the molecular photofragments produced. The method has several advantages, but foremost amongst them is that the analysis automatically yields the cross sections of interest, as a function of energy, over a very wide energy range. Another paper [17] discusses how this method may be applied to reactive scattering problems, but does not present any numerical results.

In the present work we present our first numerical attempts at applying the theory to a collinear reactive scattering problem. We demonstrate clearly that the method is capable of yielding the reaction probabilities for the production of different product quantum states over large ranges of the collision energy from the propagation of a single wavepacket. The marked resonance behaviour which has been computed for the system [18] is shown to be correctly reproduced in our calculations, though some technical problems still remain to be solved as is discussed in detail below. The time-dependent quantum mechanical treatment of reactive scattering processes has recently been extensively used to treat the  $\text{H} + \text{H}_2$  and  $\text{F} + \text{H}_2$  systems by Neuhauser et al. [19, 20]. Their methods are, however, different from those advocated here and do not yield the cross sections over the whole range of energies in as direct a manner.

## 2. Theory

In this paper we use the reaction:



with all the atoms restricted to lie on a straight line as a model reactive system to illustrate the use of time-dependent quantum dynamical techniques. The potential is taken to be Muckerman's [21] potential number 5, which is the same as that used by Schatz et al. [18]. Jacobi coordinates are used as the kinetic energy operator then possesses no cross terms [22]. With these coordinates the central problem of reactive scattering theory must be faced, namely that there are different coordinates for reactant and product arrangements, and that if, for instance, we use the Jacobi coordinates corresponding to the reactant arrangement then the product quantum state analysis is complicated by the need to transform the wavefunction into the product arrangement coordinates beforehand. In order to avoid this difficulty we use the product arrangement Jacobi coordinates throughout to perform the time propagation of the wavepacket. This in turn of course introduces some difficulty in setting up the initial wavepacket, which must first be defined in terms of the reactant Jacobi coordinates and then transformed into the product coordinates.

The initial wavepacket is created by first using the Fourier Grid Hamiltonian (FGH) method [23] to compute a grid representation of the desired  $\text{H}_2$  vibra-

tional wavefunction  $\phi_v(R_{\text{H-H}})$ . This is then multiplied by a Gaussian function in the  $R_{\text{F-H}_2}$  coordinate ( $\exp[-\alpha(R_{\text{F-H}_2} - R_{\text{F-H}_2}^0)^2]$ ). Finally the product of these two functions is multiplied by an incoming travelling wave in the  $R_{\text{F-H}_2}$  coordinate. Combining all of these elements we may write the initial wavepacket as:

$$\Phi(R_{\text{F-H}_2}, R_{\text{H-H}}, t = 0) = \exp[-ik(R_{\text{F-H}_2} - R_{\text{F-H}_2}^0)] \cdot \exp[-\alpha(R_{\text{F-H}_2} - R_{\text{F-H}_2}^0)^2] \phi_v(R_{\text{H-H}}) \quad (2)$$

In order to gain information as to the incident relative flux of molecules, which is needed to calculate the cross section or reaction probability, the initial wavepacket must be Fourier-transformed:

$$f(k_v) \phi_v(r) = \frac{1}{2\pi} \int_{R=0}^{\infty} e^{-ik_v R} \Phi(R, r, t = 0) dR \quad (3)$$

where the notation has been simplified by using  $R = R_{\text{F-H}_2}$  and  $r = R_{\text{H-H}}$ . The inverse Fourier transform, which gives back a representation of the initial wavepacket is:

$$\Phi(R, r, t = 0) = \left[ \int_{-\infty}^{\infty} f(k_v) e^{ik_v R} dk_v \right] \phi_v(r) \quad (4)$$

We see therefore that the amplitude or weight associated with that part of the wavepacket which has energy  $E = \hbar^2 k_v^2 / 2\mu + \epsilon_v$ , and which corresponds to the mutual approach of the two collision partners is  $f(|k_v|)$ .

Starting with the initial wavepacket given in Eq. (2), we first transform it to the product Jacobi coordinates and then solve the time-dependent Schrödinger equation by propagating in discrete time intervals [11–14]. The final product state asymptotic analysis may then be performed directly in these coordinates. The wavepacket is propagated forward in time in small time steps (each of about 8.2 a.u. (or 0.20 femto secs)). After each time interval the wavepacket is evaluated along a cut perpendicular to the exit valley and lying in the asymptotic region at  $R_{\text{H-HF}} = R_{\text{H-HF},\infty}$ . The coefficients,  $C_v(R_{\text{H-HF},\infty}; t)$ , required for the final state product vibrational analysis of the wavepacket are then obtained in exactly the same manner as those used in the calculation of partial photofragmentation cross sections.

$$C_v(R_{\text{H-HF},\infty}; t) = \int_0^{\infty} \phi_v(R_{\text{H-F}}) \Phi(R_{\text{H-HF},\infty}; R_{\text{H-F}}; t) dR_{\text{H-F}} \quad (5)$$

The product vibrational wavefunctions,  $\phi_v(R_{\text{H-F}})$ , are generated on a linear grid using the FGH method [23], and the integral in Eq. (5) is computed using the formula:

$$C_v(R_{\text{H-HF},\infty}; t) = \Delta R_{\text{H-F}} \sum_{i=1}^{N_v} \phi_{vi} \Phi_{J,i}(t) \quad (6)$$

where  $\Delta R_{\text{H-F}}$  is the spacing between grid points in the “ $R_{\text{H-F}}$ ” coordinate,  $\phi_{vi}$  is the value of the  $v$ th asymptotic vibrational wavefunction on the  $i$ th grid point (calculated by the FGH method [23]) and  $\Phi_{J,i}(t)$  is the value of the wavepacket on the  $J$ ,  $i$ th grid point at time  $t$ , where the  $J$ th column of the grid corresponds to the  $R_{\text{H-HF}}$  value chosen for the asymptotic analysis,  $R_{\text{H-HF}} = R_{\text{H-HF},\infty}$ . The time-dependent coefficients  $C_v(R_{\text{H-HF},\infty}; t)$  are now Fourier transformed to extract the energy dependence of the scattered wavepacket [9]:

$$A_v(R_{\text{H-HF},\infty}; E) = \frac{1}{2\pi} \int_{t=0}^{\infty} e^{iEt/\hbar} C_v(R_{\text{H-HF},\infty}; t) dt \quad (7)$$

The analysis of our previous paper [9] shows that the  $A_{v'}$  coefficients may be written as:

$$A_{v'}(R_{\text{H-HF},\infty}; E) = \hbar \cdot \left[ \frac{\mu'}{h^2 2\pi k_{v'}} \right]^{1/2} \frac{1}{2i} e^{ik_{v'} R_{\text{H-HF},\infty}} \\ \times \langle \psi_{v'}^-(R_{\text{H-HF},\infty}, R_{\text{H-HF}}; E) | \Phi(R_{\text{H-HF}}, R_{\text{H-F}}; t=0) \rangle \quad (8)$$

The scattering wavefunctions  $\psi_{v'}^-$  occur in the equation as these are the ones which correspond at large times to definite well characterised outgoing plane waves and are the appropriate time-independent functions for the analysis of the long time behaviour of a wavepacket [9, 24].

The asymptotic behaviour of the time-independent scattering wavefunction  $\psi_{v'}^-$  may be written as:

$$\psi_{v'}^-(R, r, E) \xrightarrow{R_{\text{H-HF}} \rightarrow \infty} \left[ \frac{\mu'}{h^2 2\pi k_{v'}} \right]^{1/2} \frac{1}{2i} \left\{ e^{ik_{v'} R'} \phi_{v'}(r') - \sum_f S_{v'f}^* \left[ \frac{k_{v'}}{k_f} \right]^{1/2} e^{-ik_f R'} \phi_f(r') \right\} \quad (9a)$$

$$\psi_{v'}^-(R, r, E) \xrightarrow{R_{\text{F-HH}} \rightarrow \infty} - \left[ \frac{\mu'}{h^2 2\pi k_{v'}} \right]^{1/2} \frac{1}{2i} \sum_i S_{vi}^* \left[ \frac{k_{v'}}{k_i} \right]^{1/2} e^{-ik_i R} \phi_i(r) \quad (9b)$$

where we have now simplified the notation so that  $R' = R_{\text{H-HF}}$  and  $r' = R_{\text{H-F}}$ . Equation (9a) gives the behaviour of the wavefunction in the asymptotic part of the product exit channel, while Eq. (9b) gives its behaviour in the entrance or reactant channel.

The initial wavepacket,  $\Phi(R, r, t=0)$ , must be situated entirely in the entrance channel such that its overlap with all the product vibrational wavefunctions is zero. This means that the integrand in the overlap integral,  $\langle \psi_{v'}^-(R, r, E) | \Phi(R, r, t=0) \rangle$ , in Eq. (8) is non-zero only in the asymptotic part of the reactant entrance channel and the integral therefore selects out that part of  $\psi_{v'}^-$  given in Eq. (9b). If we now substitute Eq. (9b) into the integral in Eq. (8) and utilise the orthonormality of the reactant vibrational wavefunctions  $\phi_i(r)$  we obtain:

$$A_{v'}(R'_{\infty}, E) = \frac{\hbar}{4} \cdot \left[ \frac{\mu'}{h^2 2\pi} \right] e^{ik_{v'} R'_{\infty}} S_{v'v}^* \left[ \frac{1}{k_v k_{v'}} \right]^{1/2} \\ \times \left\{ \int_{R=0}^{\infty} \int_{r=0}^{\infty} e^{-ik_v R} \phi_v(R_{\text{H-H}}) \Phi(R, r, t=0) dR dr \right\} \quad (10)$$

Note that only  $\phi_v(R_{\text{H-H}})$  appears in Eq. (10) because we have already taken account of the fact that this is the only vibrational wavefunction contributing to the initial wavepacket. Using Eq. (3) the integral in this equation may now be replaced to yield:

$$A_{v'}(R_{\infty}, E) = \frac{\mu'}{8\pi\hbar} e^{ik_{v'} R_{\infty}} S_{v'v}^* \left[ \frac{1}{k_v k_{v'}} \right]^{1/2} f(|k_v|) \quad (11)$$

This equation enables us to determine the all important scattering  $\mathcal{S}$  matrix from a knowledge of the coefficients  $A_{v'}$ . In the present collinear reactive scattering case we are interested in calculating reaction probabilities,  $P_{v,v'}$ , to compare with the exact time-independent calculations of Schatz et al. [9].

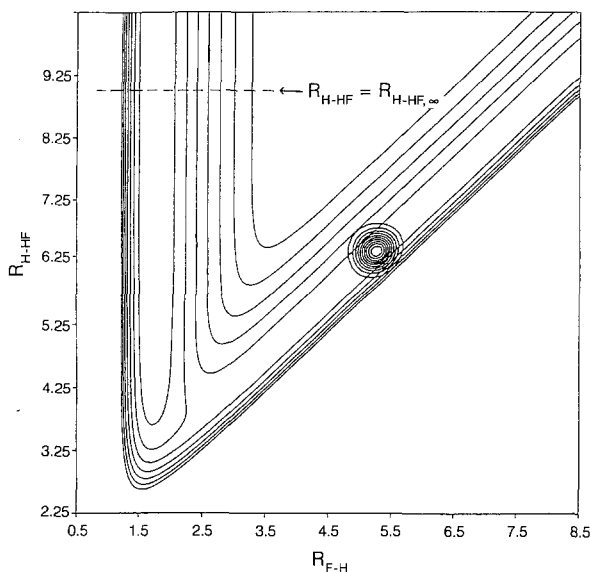
These are given by the square of the  $S$  matrix elements:

$$P_{v,v'} = |S_{v'v}|^2 = \frac{64\pi^2\hbar^2}{\mu'^2} k_{v'}k_v \left| \frac{A_{v'}(R'_\infty, E)}{f(|k_v|)} \right|^2 \quad (12)$$

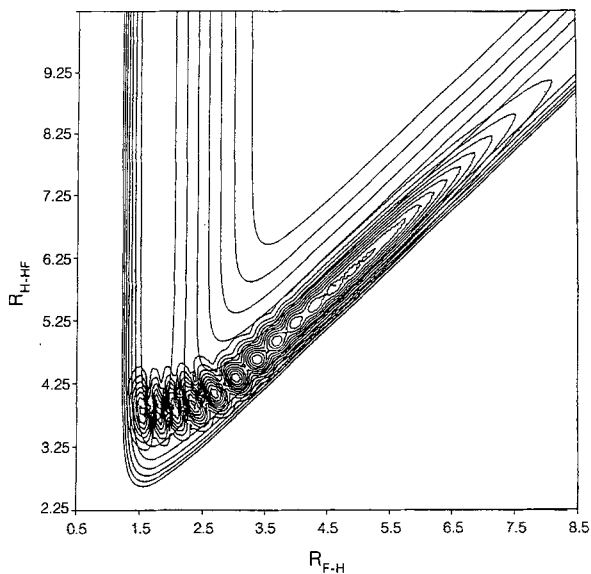
### 3. Results and discussion

Figure 1 shows contours of the absolute value of the initial wavepacket ( $t = 0$ ) superimposed on contours of the potential energy surface. The figure also shows the analysis line in the HF + H exit valley (i.e.  $R_{\text{H-HF}} = R_{\text{H-HF},\infty}$ ) along which the wavepacket is analysed at each time step. Figure 2 shows the wavepacket after it has been propagated for 14.5 femto secs (600 a.u.). It is just entering the interaction region. Figure 3 shows the wavepacket after 58 femto secs (2400 a.u.) and we see that an interesting nodal structure has developed in the interaction region. This is the signature of the strong  $v' = 2$  and  $v' = 3$  resonances which dominate the reactive scattering of this model system [18]. While Fig. 4 shows the wavepacket at an even later time when most of it has left the interaction region.

Figure 5 shows the time-dependent coefficients,  $C_{v'}(R_{\text{H-HF},\infty}; t)$ , calculated using Eqs. (5) and (6) for final vibrational states  $v' = 2$  and  $v' = 3$ , and Fig. 6 shows the reaction probabilities [Eqs. (7) and (12)] calculated from them. An important point to note is that the final state specific reaction probabilities have been obtained in a very simple manner, from a single wavepacket propagation over a very wide kinetic (or total) energies. All the major features of the scattering are present, as may be confirmed by comparison with the exact time-independent calculations of Schatz et al. [18]. There is however something fundamentally unsatisfactory about the time-dependent coefficients shown in Fig. 5. This is that they do not fall off to zero before the end of the finite time interval considered.



**Fig. 1.** Contour plot of the absolute value of the initial wavepacket ( $t = 0$ ) superimposed on a single contour of the potential energy surface. Also shown is the analysis line in the HF + H exit valley (i.e.  $R_{\text{H-HF}} = R_{\text{H-HF},\infty}$ ) along which the wavepacket is analysed at each time step



**Fig. 2.** Contour plot of the absolute value of the wavepacket at  $t = 600$  a.u. (14.5 femto secs). The wavepacket is just entering the interaction region

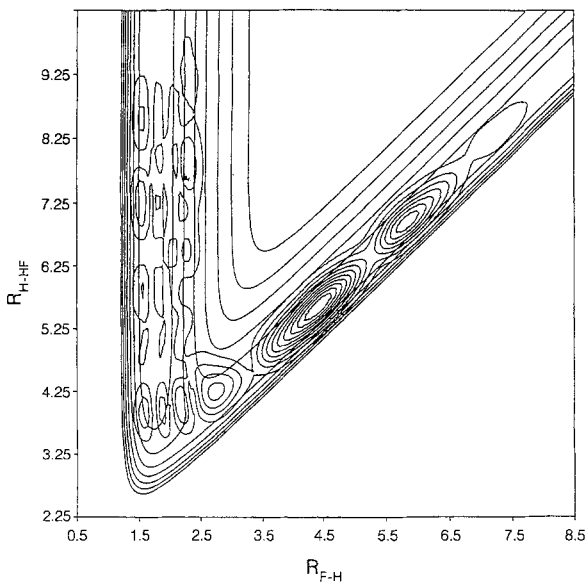


**Fig. 3.** Contour plot of the absolute value of the wavepacket at  $t = 2400$  a.u. (58.0 femto secs). The wavepacket has entered the interaction region and the nodal structure of the resonance is clearly visible

Besides the fact that this will lead to numerical problems (aliasing) and edge effects [25], it is of course physically incorrect.

We see (Fig. 5) that at large times the coefficients have ceased to decay appreciably. We attribute this to edge effects arising from the manner in which we have carried out the wavepacket propagation. After each time step of the time propagation we “damp” the edges of the grid so that the wavepacket becomes zero just before it reaches the edge. This process should avoid the problem of aliasing [25] (or false reflections) which would otherwise arise. In our previous photodissociation work [9, 10] this procedure worked well and did not give rise to any problems. As we and others [26] have discovered, however, an

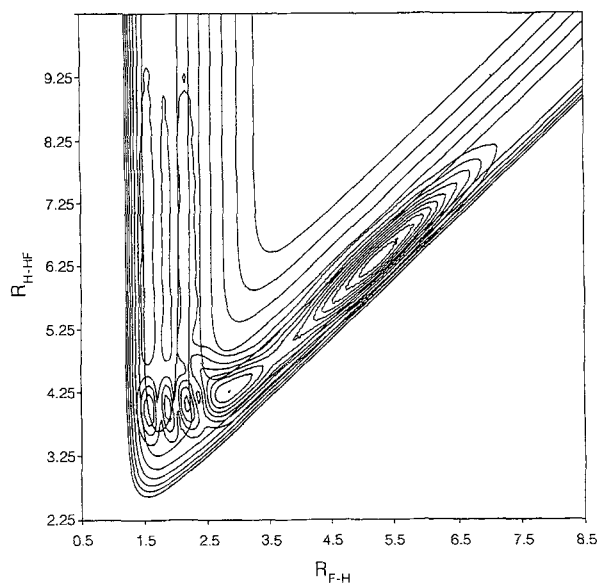


**Fig. 4.** Contour plot of the absolute value of the wavepacket at  $t = 9000$  a.u. (218 femto secs). The wavepacket has mainly left the interaction region and is proceeding down the exit valley

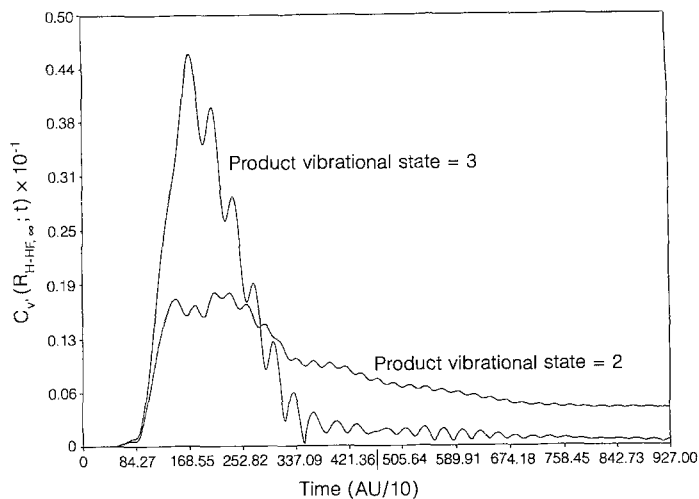


**Fig. 5.** The absolute values of the time-dependent coefficients  $C_v(R_{H-HF, \infty}; t)$  resulting from the asymptotic analysis of the wavepacket for  $v' = 2$  and  $v' = 3$

additional problem appears in reactive scattering theory. This is that the kinetic energies are smaller in this case and the associated wavelengths are longer. This means that if the damping at the edges of the grid is performed too abruptly (on a scale compared with the longest wavelength of importance) then some of the wavepacket will be (wrongly) reflected back from the damper at the edge of the grid. This appears unfortunately to be happening in the present case. Our current research efforts are directed at overcoming this difficulty in as simple a numerical and conceptual manner as possible.

Figure 7 shows a modified set of time-dependent coefficients,  $C_v(R_{H-HF, \infty}; t)$ , in which we have artificially damped down the long time tail of the coefficients (between 8000 and 16000 a.u.) so that they fall off to zero by the end of the time period considered. This procedure is analogous to windowing [25] which is often used in Fourier transform theory to reduce the consequences of edge effects.

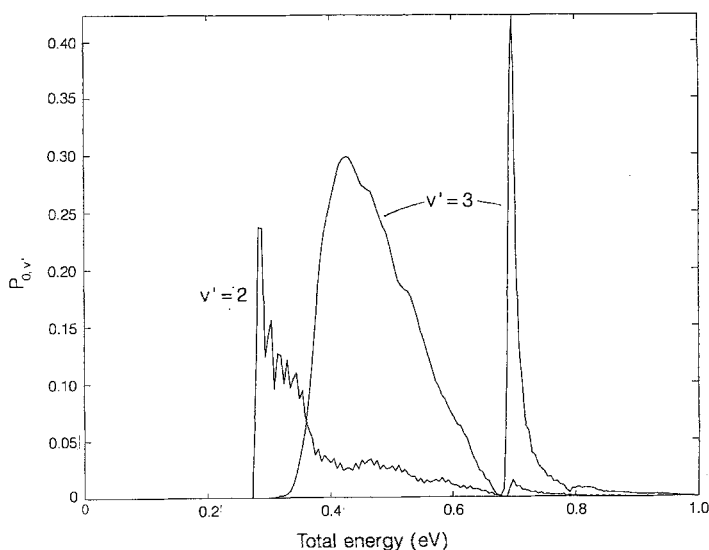


**Fig. 6.** The probabilities of reacting to produce final vibration quantum states  $v' = 2$  and  $v' = 3$  as a function of energy; see Eq. (12)

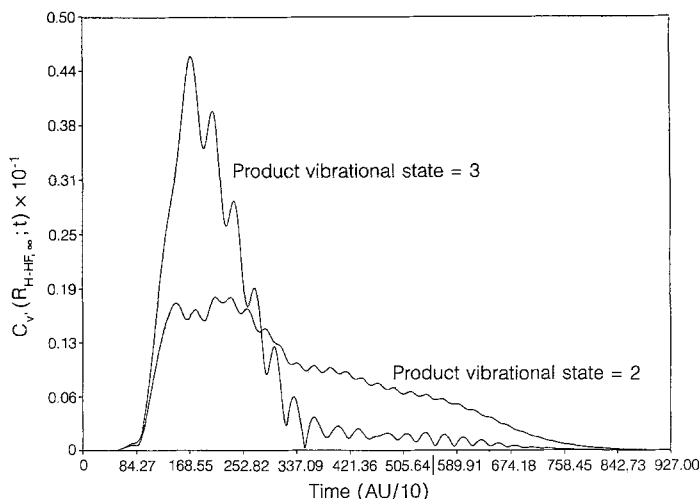


**Fig. 7.** The absolute values of the time-dependent coefficients  $C_v(R_{H-HF,\infty}; t)$  resulting from the asymptotic analysis of the wavepacket for  $v' = 2$  and  $v' = 3$ . The long time tail of the coefficients has been multiplied by an exponential damping factor (compare with Fig. 5)

Figure 8 shows the reaction probabilities for producing final vibrational quantum states  $v' = 2$  and  $v' = 3$  from  $H_2(v = 0)$  over the range of energies covered by our wavepacket. We have confirmed that the exact details of the way in which we damp the time-dependent coefficients do not have any significant effects on our results. These results compare very well with the exact time-independent quantum results of Schatz et al. [18]. All of the resonances are predicted to fall in exactly the correct places (present calculations:  $v' = 2$  resonance at 0.289 eV,  $v' = 3$  at 0.697 eV, Schatz et al. [18] obtain 0.288 and 0.695 eV). There is however slightly more structure in our reaction probability plots than in the exact (time-independent) ones [18]. This is clearly a remnant of the edge effects which have not been fully removed by our elementary windowing procedure.



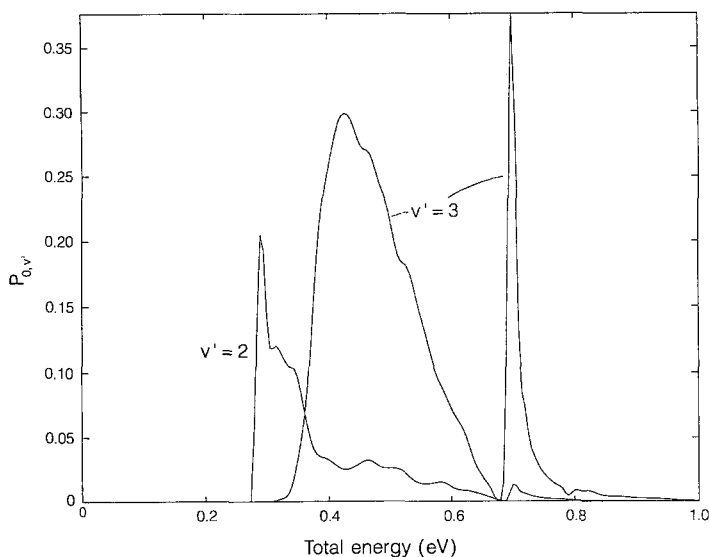


**Fig. 8.** The probabilities of reacting to produce final vibrational quantum states  $v' = 2$  and  $v' = 3$  as a function of energy [see Eq. (12)] as obtained from the damped coefficients of Fig. 7

#### 4. Conclusions

The paper has discussed the application of time-dependent quantum scattering techniques to molecular reactive scattering processes using a simple collinear system as a test case. The  $F + H_2$  system used in fact presents a very serious test for time-dependent methods as it displays sharp (i.e. long-lived) resonances which are expected to be especially difficult to treat using time-dependent techniques. Our final results (see Fig. 8) agree very well with the exact time-independent quantum calculations [18]. They reproduce all the resonance behaviour and are in good quantitative agreement with the previously reported reaction probabilities. They show slightly more structure in their energy dependence and as discussed in the text this is the result of a technical problem associated with the way in which we propagate the wavepacket and which is currently being addressed.

Our calculations illustrate the application of our new method for analysing time-dependent quantum mechanical calculations [9] to reactive scattering problems. They demonstrate, in a way which has not previously been done, the elegance and ease with which *a single time-dependent wavepacket propagation can, if properly analysed, yield final quantum state specific cross sections over a very large range of energies.*

#### References

1. Henriksen NE, Zhang J, Imre DG (1988) *J Chem Phys* 89:5607
2. Zhang J, Heller EJ, Huber D, Imre DG, Tannor D (1988) *J Chem Phys* 89:3602
3. Kulander KC, Heller EJ (1978) *J Chem Phys* 69:2439
4. Engel V, Metiu H (1989) *J Chem Phys* 91:1596
5. Weide K, Hennig S, Schinke R (1989) *J Chem Phys* 91:7630
6. Jacou M, Atabeck O, Leforestier C (1989) *J Chem Phys* 91:1585
7. Dixon RN (1989) *Molec Phys* 68:263

8. Gray SK, Wozny CE (1989) *J Chem Phys* 91:7671
9. Balint-Kurti GG, Dixon RN, Marston CC (1990) *Faraday Transactions of Chem Soc* 86:1741
10. Dixon RN, Marston CC, Balint-Kurti GG (in press) *J Chem Phys*
11. Kosloff D, Kosloff R (1983) *J Comput Phys* 52:35
12. Kosloff R, Kosloff D (1986) *J Comput Phys* 63:363
13. Tal-Ezer H, Kosloff R (1984) *J Chem Phys* 81:3967
14. Kosloff R (1988) *J Phys Chem* 92:2087
15. McCullough EA, Wyatt RE (1971) *J Chem Phys* 54:3578, 3592
16. Dirac PAM (1958) *The principles of quantum mechanics*. Oxford University Press, Oxford
17. Balint-Kurti GG, Dixon RN, Marston CC, Mulholland AJ (in press) *Comput Phys Commun*
18. Schatz GC, Bowman JM, Kuppermann A (1975) *J Chem Phys* 63:674
19. Neuhauser D, Baer M, Judson RS, Kouri DJ (1990) *J Chem Phys* 93:312
20. Neuhauser D, Baer M, Judson RS, Kouri DJ (1990) *Chem Phys Letters* 169:372
21. Muckerman JT (1981) in: Eyring H, Henderson DH (eds) *Theoretical chemistry: Advances and perspectives*, Vol 6A, Academic Press, New York, p 1
22. Sutcliffe BT, Tennyson J (1986) *Molec Phys* 58:1053
23. Marston CC and Balint-Kurti GG (1989) *J Chem Phys* 91:3571
24. Newton RG (1966) *Scattering theory of waves and particles*. McGraw-Hill, New York
25. Press WH, Flannery BP, Teukolsky SA, Vetterling WT (1986) *Numerical recipes*, Cambridge University Press, Cambridge
26. Neuhauser D, Baer M (1989) *J Chem Phys* 90:4351